Synthetic Aperture Radar for oil spill monitoring: a brief review

Andrea Buono[1]
Rafael Lemos Paes[2]
Ferdinando Nunziata[1]
Maurizio Migliaccio[1]

[1] Dipartimento di Ingegneria, Università degli Studi di Napoli Parthenope
Centro Direzionale, isola C4, 80133 – Napoli, Italy
andrea.buono, ferdinando.nunziata, maurizio.migliaccio@uniparthenope.it

[2] Instituto Nacional de Pesquisas Espaciais (INPE), Earth Observation Coordination
12227-010, São José dos Campos - SP, Brazil
rlpaes@dsr.inpe.br

Abstract. In this paper, a review of Synthetic Aperture Radar (SAR)-based techniques, for oil slick at sea observation is proposed, focusing in particular on polarimetric approaches. In fact, marine oil pollution monitoring is a topic of great applicative and scientific relevance and in such a context, among all remote sensing sensors, SAR represents a fundamental tool due to its almost all-weather and all-day imaging capability, providing synoptic maps of the observed scene with a fine spatial resolution and a dense revisit time. Although traditionally SAR-based techniques for oil pollution observation rely on automatic or partially supervised classifiers applyed on single-polarization SAR imagery and based on image processing algorithms, in the last decade the growing number of fully and partially polarimetric data available from several polarimetric SAR sensors offered an unprecedented amount of physical information about the scattering mechanisms ruling the interaction between the observed scene and the SAR illumination. Hence, a set of polarimetric approaches that exploit the oil-covered sea surface departure from Bragg scattering, which characterizes the scattering from a slightly rough surface as the slick-free ocean one, have been developed. Polarimetric SAR observations represent a significant improvement allowing to distinguish oil slicks from look-alikes (low-wind areas, biogenic films, etc.) and to avoid or reduce the need of trained personnel and external information (optical and scatterometer data) required for single polarization SAR-based techniques.

Keywords: synthetic aperture radar, polarimetry, oil spill .

1. Introduction

Oil pollution is a matter of great concern: every year 180 millions US gallon of crude oil are spilled into the sea (DELILAH, 2002; ITOPF, 2007). Spilled oil modifies marine ecosystems altering fish life-cycle with hard aftermaths for human health. Mineral oil spills are mainly due to intentional polluters, i.e., vessels which get benefits in illegally discharging oil waste (oily ballast waters, tank washing residues, fuel oil sludge and bilge discharges) (UNEP2014, 2014), or to accidental disasters as the Transocean Deepwater Horizon (Gulf of Mexico, 20 April 2010) and the Prestige (Galician coast, 19 November 2002) cases. In 2013, 7 spills of at least 60 US gallon of various mineral oil types have been recorded, 3 of which have been reported as large spill (> 6,000 US gallon). Nonetheless, historical databases show a decreasing trend for large oil spills (from, in average, 25 large oil spills occurred in the decade 1970-1979 to the 5 recorded in the 2000-2009 decade), while the majority (81%) of the nearly 10,000 annual accidents falls into the smallest category (< 60 US gallon) (ITOPF, 2013). Those considerations witness that a continous and effective oil spill surveillance is needed to effectively plan proper and timely

countermeasures to minimize pollution effects, i. e., the use of dispersants, and to operationally support law enforcement and early warning systems for hazards management, catching in the act the polluters and timely identify them to be prosecuted.
The remainder of the paper is organized as follows: in Section 2, a brief review of the single polarization Synthetic Aperture Radar (SAR)-based remote sensing for oil pollution monitoring, together with the rationale lying at the basis of SAR capability to observe oil slicks over ocean surface is presented, describing the most employed single polarization techniques that have been proposed in literature with their underpinning ideas, especially focusing on main drawbacks that have to be taken in account when dealing with single polarization SAR imagery; in Section 3, the theoretical background on which rely polarimetric SAR-based approaches for oil slick observation is described, analyzing in detail the set of the most used polarimetric features and discussing their capability to detect and classify oil slicks; conclusions are drawn in Section 4.

2. Single Polarization SAR-based oil spill observation

Spaceborne remote sensing and aerial surveillance represent key tools for an operational oil pollution monitoring. In fact, when dealing with oil slick at sea observation, a wide area coverage together with a fine spatial resolution and a dense revisit time are required to monitor huge marine areas in case of oil fields or large oil spills, to ensure a timely identification of illegal polluters and to plan proper countermeasures. From this point of view, being a microwave, active and coherent high-resolution imaging sensor, SAR represents a non-cooperative system that can operate almost independently on atmospheric conditions (rain, cloud-cover) allowing day- and night-time measurements perfectly matching the aforementioned constraints and overcoming traditional issues of in situ techniques (i. e., coast guard and surveillance aircrafts), usually non cost-effective. Nevertheless, it should be underlined that although SAR ensures a very improved spatial/temporal coverage providing, after proper processing, synoptic maps of the observed area (MIGLIACCIO et al., 2012), it can not provide reliable estimates of oil thickness.
Basically, SAR can observe oil slicks over the ocean surface due to the oil capability to reduce the friction velocity, responsible of the energy exchanges between sea surface wind and ocean waves, and to dampen the short gravity and capillary waves, i. e., the Bragg resonant centimetric waves responsible of the backscattering signal measured at the SAR antenna (MIGLIACCIO; GAMBARDELLA; TRANFAGLIA, 2007). Hence, the reduced ocean surface roughness results in a low backscattered region appearing, in gray-scale SAR imagery, as a darker area with respect to the sea background. Operationally, SAR-based oil pollution monitoring can be achieved only when low-to-moderate wind conditions apply (wind speed between 3 and 15 m/s (BREKKE; SOLBERG, 2005)). In fact, wind speed has to be sufficiently high to produce ocean waves responsible of backscattering, but not too strong to avoid producing dispersion and water/oil mixing phenomena that make thin oil slicks at sea practically invisible. Nonetheless, low-wind ocean areas (LW) are characterized by very small surface roughness that similarly results in dark patches in SAR imagery. Furthermore, there is a large variety of features, termed look-alikes and including rain cells (RC), ship wakes (SW), oceanic currents (C), biogenic surfactants, upwelling zones, etc. that for different reasons appear as dark areas in SAR imagery producing false positives (FINGAS; BROWN, 1997; MIGLIACCIO; GAMBARDELLA; TRANFAGLIA, 2007; NUNZIATA; SOBIESKI; MIGLIACCIO, 2009). In Fig. 1 some examples of look-alikes are shown. They hamper the visual interpretation of SAR imagery making oil pollution monitoring based on single polarization SAR data a very non trivial task, although in some cases the expertise of trained personnel or the use of external ancillary information, i.e., scatterometer local wind measurements and optical data, can strongly support it.

Historically, single polarization SAR-based techniques address oil slicks monitoring using an image processing approach based on a 3-step procedure (MIGLIACCIO; GAMBARDELLA; TRANFAGLIA, 2007; GAMBARDELLA et al., 2010), as shown in Fig. 2(a). Once detected dark areas possible candidates to be oil spills using segmentation, active contours tracing or neural network-based alghoritms (FRATE et al., 2000; SINGHA; BELLERBY; TRIESCHMANN, 2013; GARCIA-PINEDA et al., 2013; HUIHUI; BO; KAIHUA, 2013; TARAVAT; LATINI; FRATE, 2014), an unsupervised or partially supervised classifier is accomplished. It is based on the computation of a set of radiometric, geometric and texture features extracted to assign a certain probability that the considered dark area is a on oil spill. The key point relies in the features set choosen to analyze the morphological complexity of dark patches (SOLBERG, 2012), which depends on oil composition, amount and shape, on the kind of the releasing source (stationary as drilling platforms and pipelines or moving as tankers and vessels) and on weather conditions as sea surface temperature, wind field and oceanic currents. In particular, weather conditions play an important role in the life-cycle of the oil spill ruling processes like evaporation, emulsification and dispersion (SOLBERG et al., 1999). In Fig. 2(b)-(d) typical outputs of automatic classifiers are shown. However, it is important to underline that such classifiers, sometimes referred as automatic, in real cases have to be supported with external information (about the local wind field and the sea state from scatterometer or buoy data, and about the accurate location of metallic targets within the observed scene) to be reliable for a timely and effective oil spill detection, and in few cases they are able to discriminate oil slicks from look-alikes. Hence, although sometimes unsupervised, they often need the expertise of trained personnel providing visual inspection. Moreover, no physical characterization or a very limited one is integrated in the processing chain. More details regarding the automatic classifiers for oil spill detection purposes that have been proposed in literature can be found in (SOLBERG et al., 1999; BREKKE; SOLBERG, 2005; NIRCHIO, 2005; KERAMITSOGLOU; CARTALIS; KIRANOUDIS, 2006; MERCIER; GIRARD-HARDUIN, 2006; SOLBERG; BREKKE; HUSOY, 2007; BREKKE; SOLBERG, 2008; GAMBARDELLA et al., 2010).
In literature, a completely different rationale has been followed for oil slick detection and classification from single polarization SAR imagery. It has a physical nature relying in statistical or scattering models of the ocean surface which account for slick-free and a slick-covered sea surface scenarios. In (MIGLIACCIO; GAMBARDELLA; TRANFAGLIA, 2007), a 3-parameters distribution family, namely the Generalized-K, is employed to model the speckle of low backscattering areas in Single-Look Complex (SLC) SAR data. Although such a model allows to detect dark areas, it is not able to provide an oil/look-alike discrimination and its performance stongly depend on the statistical parameters estimation. In (NUNZIATA; SOBIESKI; MIGLIACCIO, 2009), a 2-scale approach to model the sea surface scattering with and without oil slicks is followed and validated over C- and L-band Multi-Look Complex (MLC) SAR data using the Boundary Perturbation Model (BPM) as a good benchmark between accuracy and time-consuming. It provides a contrast model which predicts an oil slick backscattering lower than the surrounding slick-free background due to the capability of an oil slick to reduce the ocean surface roughness and the friction velocity, shortening the sea spectrum and shrinking the statistical distribution of the slopes.

3. Polarimetric SAR-based techniques for oil spills monitoring

In last decade, the growing availability of dual- and full-polarimetric data from a set of airborne and spaceborne SAR sensors operating at different frequencies and polarizations allowed the strong development of polarimetric models and analysis tools to observe oil slicks at sea. In literature, spaceborne and airborne full-polarized L-band SAR acquisitions from

the Japanese ALOS-PalSAR (MIGLIACCIO et al., 2009) and the NASA UAVSAR (MINCHEW; JONES; HOLT, 2012), respectively, full-polarized C-band measurements from the Canadian RADARSAT-2 (MIGLIACCIO et al., 2011a; ZHANG et al., 2011) and dual-polarized X-band data from the German TerraSAR-X (VELOTTO et al., 2011) have been exploited for this purpose since they provide an unprecedented amount of information about the scattering mechanisms of the observed scene, allowing the classification of dark areas in single polarization SAR imagery (MIGLIACCIO; GAMBARDELLA; TRANFAGLIA, 2007; MIGLIACCIO et al., 2011b, 2012). Several polarimetric features measuring the correlation between the co-polarized HH and VV channels, the amount of unpolarized backscattered energy, the scene depolarization capabilities, etc. have been successfully employed to both observe oil slicks and distinguish them from weak damping look-alikes. They all share a common physical rationale relying on the different scattering mechanisms ruling the electromagnetic behaviour of oil-covered and weak damping slick-covered sea surface under low-to-moderate wind conditions and for intermediate angles of incidence. In detail, sea surface scattering is well described by the Bragg or tilted-Bragg model while a strong departure from Bragg scattering is in place when dealing with oil-covered sea surface. Hence, the polarimetric features measure such a departure from Bragg scattering that is in place over oil areas having, thus, the capability to distinguish them from weak damping look-alikes since they call for a scattering mechanism very close to the Bragg one.
All the polarimetric features can be estimated directly from the measured scattering matrix $\mathbf{S}$ or using more powerful second-order models based on the coherency or covariance matrices, $\mathbf{T}$ and $\mathbf{C}$ respectively, or on the incoherent Kennaugh or Mueller matrices, $\mathbf{K}$ and $\mathbf{M}$ respectively (NUNZIATA; GAMBARDELLA; MIGLIACCIO, 2012). The coherent approach allows to define, using the Cloude-Pottier target decomposition (CLOUDE; POTTIER, 1996) some important polarimetric features, namely the target entropy H, the anisotropy coefficient A and the mean scattering angle $\bar{\alpha}$ (SKRUNES; BREKKE; ELTOFT, 2014), the degree of polarization p (NUNZIATA; GAMBARDELLA; MIGLIACCIO, 2013) and the covariance scaling factor Γ_C (SKRUNES; BREKKE; ELTOFT, 2012). Following the incoherent approach, instead, the normalized pedestal height NP, that represents the amount of unpolarized backscattered energy on which the Normalized Radar Cross Section (NRCS) is set in a 3-D plot of the synthetized NRCS as a function of ellipticity and orientation angles, namely the co-polarization signature (NUNZIATA; MIGLIACCIO; GAMBARDELLA, 2011), can be defined. Furthermore, exploiting the symmetry properties of the Mueller matrix applying when dealing with natural scenarios, i.e., slick-free or weak damping slick-covered sea surface, it can be obtained an easily interpretable binary output in which Bragg and no-Bragg regions are practically non-overlapped, avoiding any problem regarding the selection of an external threshold (NUNZIATA; GAMBARDELLA; MIGLIACCIO, 2008). Nevertheless, in literature other polarimetric parameters, directly obtainable from $\mathbf{S}$, have been proposed and tested with respect their capability to observe oil slicks at sea: the standard deviation of the Co-polarized Phase Difference (CPD) σ_{CPD} (MIGLIACCIO; NUNZIATA; GAMBARDELLA, 2009), the co-polarized correlation coefficient $\rho_{HH/VV}$, the co-polarization power ratio $\gamma_{HH/VV}$ (SKRUNES; BREKKE; ELTOFT, 2014) and the conformity parameter μ (ZHANG et al., 2011), the latter having the same implicit thresholding benefit. It has been widely demonstrated that this polarimetric feature set is suitable for oil pollution monitoring purposes. In Fig. 3(a)-(d) some certified oil slicks and look-alikes are shown with the corresponding output referred to different polarimetric approaches. In Fig. 3(e) the most commonly employed polarimetric features are summarized, together with their expected behaviour when dealing with a slick-free or a weak damping slick-covered sea surface and an oil slick-covered sea one. In Fig. 4 results witnessing the capability of other polarimetric features to emphasize the presence of oil slicks at sea and to distinguish them from look-alikes are shown. However,

it is important to underline that although polarimetric measurements provide significantly valuable information about the oil slicks physical properties, it is not a straightforward task since the signatures of oil pollutants in polarimetric SAR imagery is strongly influenced by weathering processes as spreading, drift, evaporation, emulsification, dissolution, dispersion, sedimentation, biodegradation, etc. Hence, oil slicks polarimetric characterization in terms of their damping properties, thickness and water mixing is very challenging (MINCHEW, 2012).

4. Conclusions

In this paper, a brief review of SAR-based techniques for oil slick at sea observation is proposed. Traditionally, in single-polarization SAR imagery oil pollution monitoring is performed using image processing algorithms that lie at the basis of unsupervised or partially supervised classifiers. The latter are implemented in a 3-step procedure in which a set of radiometric and geometric features are extracted from dark areas to assign a certain probability to each of them to be an oil slick. However, such techniques does not allow the discrimination between oil slicks and look-alikes, often needed external information or the expertise of trained personnel. Since in the last decade a large fully- and partially-polarimetric dataset is available, polarimetric approaches have been developed exploiting the unprecedented amount of physical information about the scattering mechanisms of the observed scene it provide. Hence, a set of polarimetric features accounting for oil-covered and oil-free sea surface, have been successfully tested to be able to measure the departure from sea Bragg scattering that is in place when dealing with oil slicks. Furthermore, on this basis, their capability to distinguish oil slicks from look-alikes, calling for a scattering very close to the Bragg mechanism, has been demonstrated.

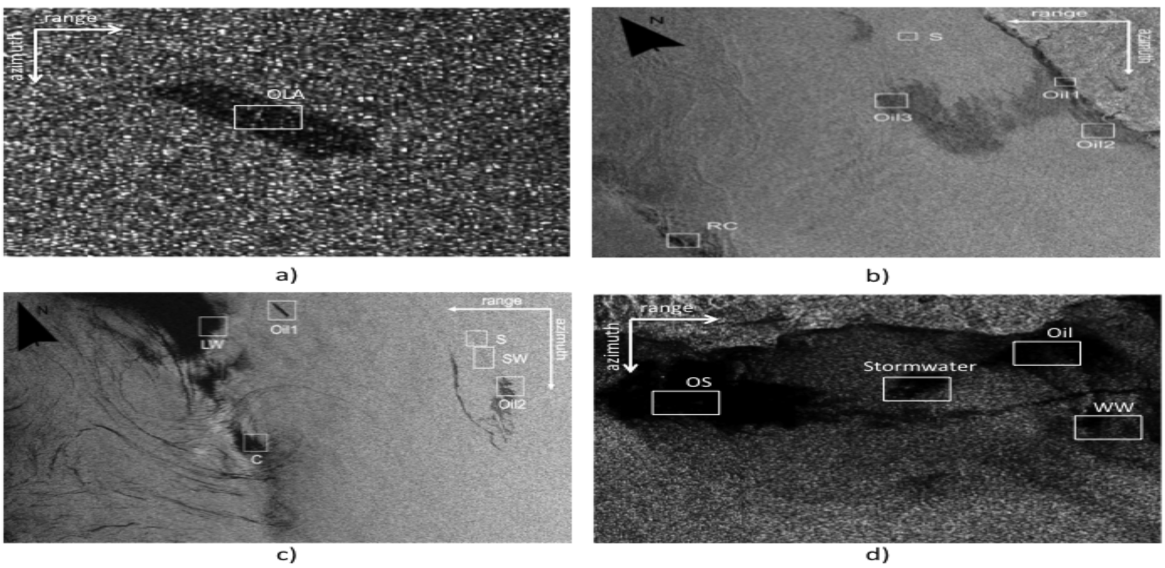

Figura 1: Oil slicks and lookalikes in single-polarization SAR imagery. VV power image relevant to the C-band MLC SIR-C/X-SAR data acquired in April 15, 1994, p.n. 11 588, in which an Oleyl alcohol LookALike (OLA) is present (a). ERS-1 SLC SAR quick-look image relevant to the acquisition of October 4, 1994 at 11:20:00Z, in which a mineral oil slick is present, together with a rain cell (RC) in the bottom left corner of the image (b). ERS-1 SLC SAR quick-look image relevant to the acquisition of July 16, 1992 at 9:52:00Z, in which is highlighted the presence, in the SAR image, of a low-wind area (LW) on the top, a ship (S) with its wake (SW) on the right side, and a low-backscetter region ruled by oceanic currents (C) in the center (c). VV-polarized squared modulus (in dB) Radarsat-2 SAR data related to the acquisition of 14 December, 2009 at 14:09:15 UTC (ID:PDS_00886040), in which can be identified a large oil seep (OS) on the left side of the image, and regions likely affected by stormwater and wastewater (WW) (d).

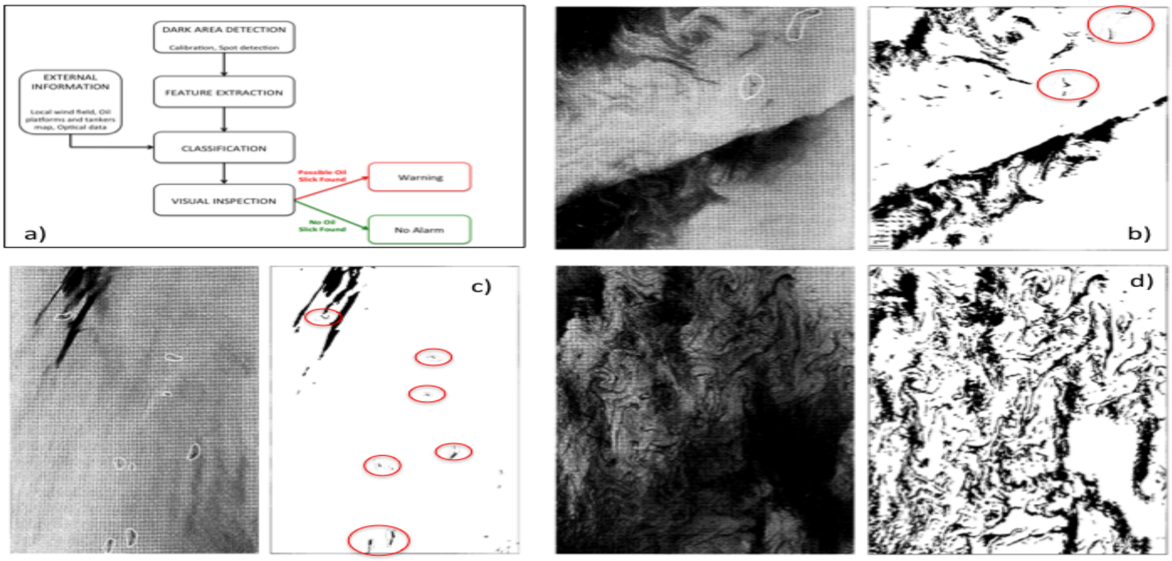

Figura 2: (a) Automatic oil spill detection in single-polarization SAR imagery. Sketch of a conventional partially supervised integrated system to support oil spill monitoring. (b), (c) ERS-1 SAR images in which several correctly classified slicks as oil connected to point sources. (d) A complex marine scenario relevant to an ERS-1 SAR acquisition in which the classifier provides no alarms. Pictures (b), (c) and (d) are from (SOLBERG et al., 1999).

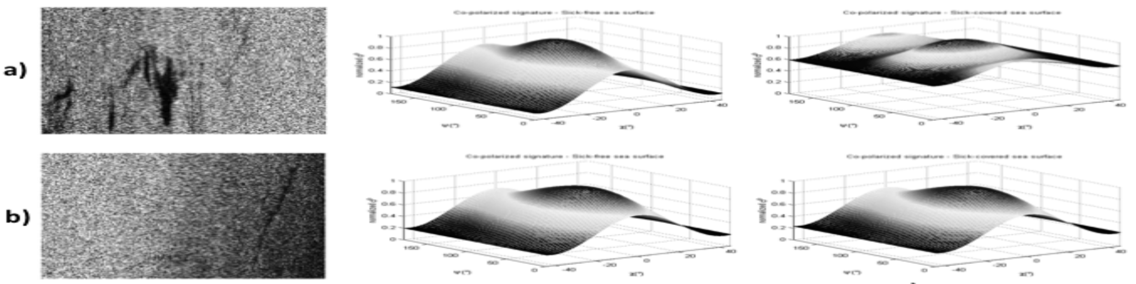

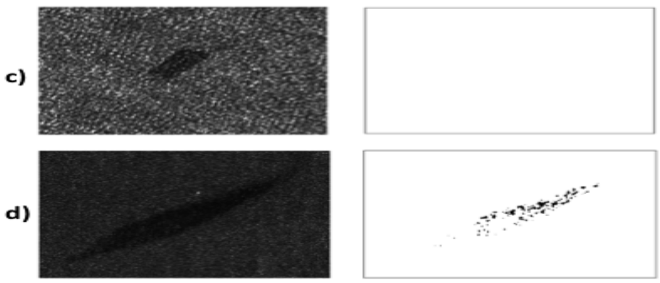

e)

POLARIMETRIC FEATURE	OIL	SEA & LOOK-ALIKE
H	HIGH	LOW
A	LOW	HIGH
$\bar{\alpha}$	MEDIUM	LOW
NP	HIGH	LOW
p	LOW	HIGH
r_c	LOW	MEDIUM
μ	> 0	< 0
σ_{CPD}	HIGH	LOW
$\rho_{HH/VV}$	LOW	HIGH
$\gamma_{HH/VV}$	LOW	MEDIUM

Figura 3: (a) On the left, an excerpt of the VV channel intensity image related to a dual-pol L-band ALOS-PalSAR acquisition (product id: ALPSRP031440190), where an oil slick is visible; on the right, the co-polarization signature for the slick-free and the slick-covered sea surface, respectively. (b) The same of (a), for the dual-pol L-band ALOS-PalSAR measure (product id: ALPSRP059890330) in which a look-alike is present. (c) On the left, an excerpt of the VV power image related to a fully-polarimetric C-band SIR-C/X acquisition (processing number 41370), where a look-alike is visible; on the right, the binary output provided by the direct comparison of two elements of the Mueller matrix. (d) The same of (c), for the fully-polarimetric C-band SIR-C/X measure (processing number 49939) in which an oil slick is present. (e) Summary table of the most commonly used set of polarimetric features for oil pollution monitoring, together with their expected behaviour over oil and sea/look-alike regions. Pictures (a) and (b) are from (NUNZIATA; MIGLIACCIO; GAMBARDELLA, 2011), (c) and (d) (NUNZIATA; GAMBARDELLA; MIGLIACCIO, 2008).

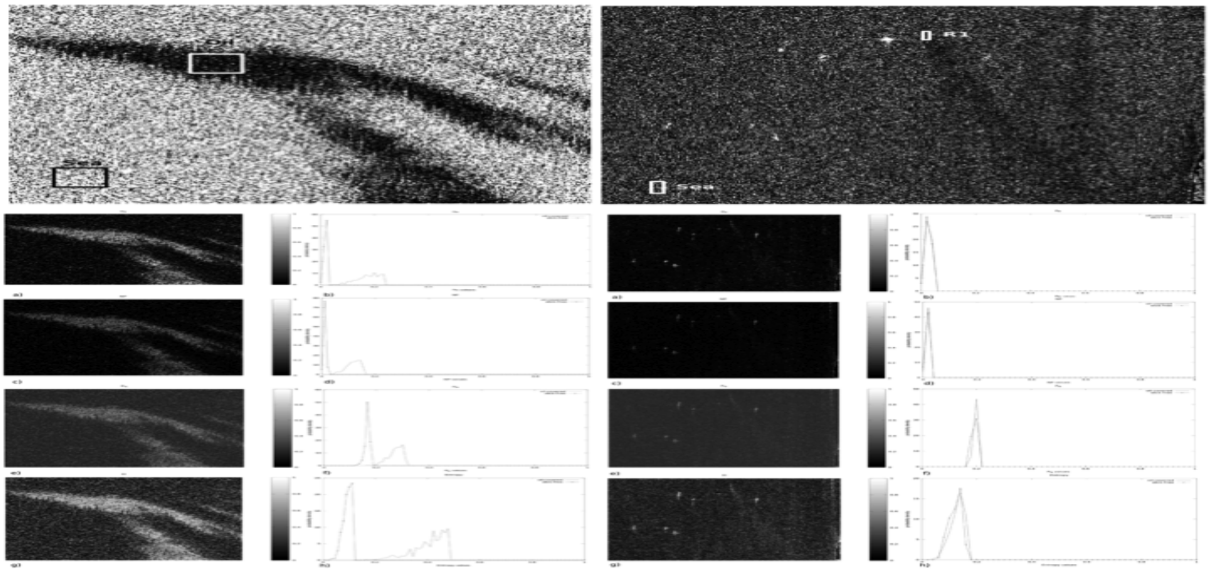

Figura 4: On the top, two polarimetric SAR images. Left: excerpt of the VV channel intensity image related to a fine quad-pol mode C-band Radarsat-2 SAR acquisition (product id: PDS01141690), where an oil slick is present; right: excerpt of the VV channel intensity image related to a dual-pol L-band ALOS-PalSAR acquisition (product id: ALPSRP095800900), where a look-alike is visible. On the bottom, polarimetric features with the corresponding empirical distributions. Top-down: grey-scaled 1-σ_{CPD}, 1-NP, 1-p and H images and their empirical pdfs. Pictures are from (NUNZIATA; GAMBARDELLA; MIGLIACCIO, 2012).

Referências

BREKKE, C.; SOLBERG, A. Oil spill detection by satellite remote sensing. *Remote Sens. Environ.*, v. 95, n. 1, p. 13, 2005.

BREKKE, C.; SOLBERG, A. Classifiers and confidence estimation for oil spill detection in envisat asar images. *IEEE Geosci. Remote Sens. Lett.*, v. 5, n. 1, p. 65–69, 2008.

CLOUDE, S. R.; POTTIER, E. A review of target decomposition theorems in radar polarimetry. *IEEE Trans. Geosci. Remote Sens.*, v. 34, p. 498–518, 1996.

DELILAH, A. *Marine oil pollution: technologies and methodologies for detection and early warning*. [S.l.], 2002. EUR 20231 EN.

FINGAS, M. F.; BROWN, C. E. Review of oil spill remote sensing. *Spill Sci. Technol. Bull.*, v. 4, p. 199–208, 1997.

FRATE, F. D. et al. Neural networks for oil spill detection using ers-sar data. *IEEE Trans. Geosci. Remote Sens.*, v. 38, n. 5, p. 2282–2287, 2000.

GAMBARDELLA, A. et al. A one-class classification for oil spill detection. *Pattern Analysis App. J.*, v. 13, p. 349–366, 2010.

GARCIA-PINEDA, O. et al. Oil spill mapping and measurement in the gulf of mexico with textural classifier neural network algorithm (tcnna). *IEEE J. Select. Topics App. Earth Obs. Remote Sens.*, v. 6, n. 6, p. 2517–2525, 2013.

HUIHUI, S.; BO, H.; KAIHUA, Z. A globally statistical active contour model for segmentation of oil slick in sar imagery. *IEEE J. Select. Topics App. Earth Obs. Remote Sens.*, v. 6, n. 6, p. 2402–2409, 2013.

ITOPF. *Baird Maritime:The International Tanker Owners Pollution Federation Limited (ITOPF) Handbook*. [S.l.], 2007. London, UK.

ITOPF. *The International Tanker Owners Pollution Federation Limited (ITOPF), Oil Tanker Spill Statistics 2013*. [S.l.], 2013. London, UK.

KERAMITSOGLOU, F.; CARTALIS, C.; KIRANOUDIS, C. Automatic identification of oil spills on satellite images. *Environ. Model. Softw.*, v. 44, n. 10, p. 2839–2846, 2006.

MERCIER, G.; GIRARD-HARDUIN, F. Partially supervised oil-slick detection by sar imagery using kernel expansion. *IEEE Trans. Geosci. Remote Sens.*, v. 44, n. 10, p. 2839–2846, 2006.

MIGLIACCIO, M. et al. The palsar polarimetric mode for sea oil slick observation. *IEEE Trans. Geosci. Remote Sens.*, v. 47, n. 12, p. 4032–4041, 2009.

MIGLIACCIO, M.; GAMBARDELLA, A.; TRANFAGLIA, M. Sar polarimetry to observe oil spills. *IEEE Trans. Geosci. Remote Sens.*, v. 45, p. 506–511, 2007.

MIGLIACCIO, M. et al. Polarimetric synthetic aperture radar utilized to track oil spills. *Trans. on EOS*, v. 93, p. 161–163, 2012.

MIGLIACCIO, M.; NUNZIATA, F.; GAMBARDELLA, A. On the co-polarised phase difference for oil spill observation. *IJRS Int. J. Remote Sens.*, v. 30, p. 1587–1602, 2009.

MIGLIACCIO, M. et al. Marine added-value products using radarsat-2 fine quad-polarization. *Can. J. Remote Sens.*, v. 37, n. 5, p. 443–451, 2011.

MIGLIACCIO, M. et al. A multi-frequency polarimetric sar processing chain to observe oil fields in the gulf of mexico. *IEEE Trans. Geosci. Remote Sens.*, v. 47, p. 4729–4737, 2011.

MINCHEW, B. Determining the mixing of oil and sea water using polarimetric synthetic aperture radar. *Geophysical Research Letters*, v. 39, n. L16607, 2012.

MINCHEW, B.; JONES, C. E.; HOLT, B. Polarimetric analysis of backscatter from the deepwater horizon oil spill using l-band synthetic aperture radar. *IEEE Trans. Geosci. Remote Sens.*, v. 50, n. 10, 2012.

NIRCHIO, F. Automatic detection of oil spills from sar images. *IJRS Int. J. Remote Sens.*, v. 26, p. 1157–1174, 2005.

NUNZIATA, F.; GAMBARDELLA, A.; MIGLIACCIO, M. On the mueller scattering matrix for sar oil slick observation. *IEEE Geosci. Remote Sens. Lett.*, v. 5, p. 691–695, 2008.

NUNZIATA, F.; GAMBARDELLA, A.; MIGLIACCIO, M. A unitary mueller-based view of polarimetric sar oil slick observation. *IJRS Int. J. Remote Sens.*, v. 33, n. 20, p. 6403–6425, 2012.

NUNZIATA, F.; GAMBARDELLA, A.; MIGLIACCIO, M. On the degree of polarization for sar sea oil slick observation. *ISPRS J. Photogrammetry Remote Sens.*, v. 78, p. 41–49, 2013.

NUNZIATA, F.; MIGLIACCIO, M.; GAMBARDELLA, A. Pedestal height for oil spill observation. *IET Radar Sonar and Navigat.*, v. 5, n. 2, p. 103–110, 2011.

NUNZIATA, F.; SOBIESKI, P.; MIGLIACCIO, M. The two-scale bpm scattering model for sea biogenic slicks contrast. *IEEE Trans. Geosci. Remote Sens.*, v. 47, n. 7, p. 1949–1969, 2009.

SINGHA, S.; BELLERBY, T.; TRIESCHMANN, O. Satellite oil spill detection using artificial neural networks. *IEEE J. Select. Topics App. Earth Obs. Remote Sens.*, v. 6, n. 6, p. 2355–2363, 2013.

SKRUNES, S.; BREKKE, C.; ELTOFT, T. A comprehensive analysis of polarimetric features for oil spill characterisation. In: *Proceedings of SEASAR*. [S.l.: s.n.], 2012.

SKRUNES, S.; BREKKE, C.; ELTOFT, T. Characterization of marine surface slicks by radarsat-2 multipolarization features. *IEEE Trans. Geosci. Remote Sens.*, v. 52, n. 9, p. 5302–5319, 2014.

SOLBERG, A.; BREKKE, C.; HUSOY, P. Oil spill detection in radarsat and envisat sar images. *IEEE Trans. Geosci. Remote Sens.*, v. 45, n. 3, p. 746–755, 2007.

SOLBERG, A. et al. Automatic detection of oil spills in ers sar images. *IEEE Trans. Geosci. Remote Sens.*, v. 37, n. 4, p. 1916–1924, 1999.

SOLBERG, A. H. S. Remote sensing of ocean oil-spill pollution. In: *Proceedings of the IEEE*. [S.l.: s.n.], 2012. v. 100, n. 10, p. 2931–2945.

TARAVAT, A.; LATINI, D.; FRATE, F. D. Fully automatic dark-spot detection from sar imagery with the combination of nonadaptive weibull multiplicative model and pulse-coupled neural networks. *IEEE Trans. Geosci. Remote Sens.*, v. 52, n. 5, p. 2427–2435, 2014.

UNEP2014. *Mediterranean Action Plan for the Barcelona Convention: Maritime traffic*. [S.l.], 2014.

VELOTTO, D. et al. Dual-polarized terrasar-x data for oil spill observation. *IEEE Trans. Geosci. Remote Sens.*, v. 30, p. 1587–1602, 2011.

ZHANG, B. et al. Mapping sea surface oil slicks using radarsat-2 quad-polarization sar image. *Geophysical Research Letters*, v. 38, 2011.